Development 140, 1282-1291 (2013) doi:10.1242/dev.086918

Drosophila p53-related protein kinase is required for PI3K/TOR pathway-dependent growth

Consuelo Ibar, Vicente F. Cataldo, Constanza Vásquez-Doorman*, Patricio Olguín‡ and Álvaro Glavic§

SUMMARY

Cell growth and proliferation are pivotal for final organ and body size definition. p53-related protein kinase (Bud32/PRPK) has been identified as a protein involved in proliferation through its effects on transcription in yeast and p53 stabilization in human cell culture. However, the physiological function of Bud32/PRPK in metazoans is not well understood. In this work, we have analyzed the role of PRPK in *Drosophila* development. *Drosophila* PRPK is expressed in every tissue analyzed and is required to support proliferation and cell growth. The Prpk knockdown animals show phenotypes similar to those found in mutants for positive regulators of the PI3K/TOR pathway. This pathway has been shown to be fundamental for animal growth, transducing the hormonal and nutritional status into the protein translation machinery. Functional interactions have established that Prpk operates as a transducer of the PI3K/TOR pathway, being essential for TOR kinase activation and for the regulation of its targets (S6K and 4E-BP, autophagy and bulk endocytosis). This suggests that Prpk is crucial for stimulating the basal protein biosynthetic machinery in response to insulin signaling and to changes in nutrient availability.

KEY WORDS: TOR pathway, Cell growth, Prpk, Apoptosis, *Drosophila*

INTRODUCTION

In multicellular organisms, cell growth, proliferation and apoptosis control body size (reviewed by Danial and Korsmeyer, 2004; Sherr, 2004). The coordination of these processes allows the correct execution of morphogenetic programs and their malfunction has been documented to be central in cancer (reviewed by Guertin and Sabatini, 2007). In vertebrates and invertebrates, insulin and its downstream pathways (phosphatidylinositol-3-kinase/Target Of Rapamycin, PI3K/TOR) play important roles in organ and cell growth controlling protein and lipid biosynthesis (Saltiel and Kahn, 2001; Efstratiadis, 1998; Leevers et al., 1996; Weinkove et al., 1999; van Sluijters et al., 2000; Dufner and Thomas, 1999).

Briefly, upon activation, the Insulin receptor recruits the Chico/IRS adaptor protein, which enables the phosphorylation of the class A PI3-kinase (Stocker and Hafen, 2000). The stimulation of PI3K increases the levels of phosphatidylinositol (3,4,5) trisphosphate at the plasma membrane, which in turn relocates and, in combination with PDK1, activates the Ser/Thr kinase Akt1/PKB. Akt1/PKB controls protein synthesis in two ways: first, through phosphorylation of FOXO transcription factor, it restricts the expression of 4E-BP, an inhibitory partner of elongation factor 4E; second, it reduces the activity of the tuberous sclerosis complex (Tsc1 and Tsc2), a negative regulator of TOR kinase, which increases GTP-Rheb level, ultimately activating TOR complex 1 (TORC1) (reviewed by Oldham and Hafen, 2003). TORC1 activity further improves translation by phosphorylating S6K (S6 ribosomal protein phosphorylating kinase) and 4E-BP. Together, these modifications drive efficient translation of 5′-TOP and cap-containing RNAs (Miron et al., 2001). Besides its control by insulin, TORC1 activity depends on nutrient availability. Thus, reduced amino acid levels diminish TORC1 activity, leading to macroautophagy as protective response (Colombani et al., 2003; Scott et al., 2004). In addition, recent studies have identified the influence of TOR on bulk endocytosis, as well as its reciprocal relation in the control of cell growth and autophagy (Hennig et al., 2006).

Yeast pID261/Bud32 is an atypical Ser/Thr kinase conserved throughout metazoans and required for normal cell growth and survival (Abe et al., 2001; Facchin et al., 2002b; Facchin et al., 2002a). Studies in *S. cerevisiae* have uncovered two fundamental roles for Bud32: as a constituent of the KEOPS complex (kinase, putative endopeptidase and other proteins of small size), a regulator of telomere structure (Downey et al., 2006); and as a part of the EKC (endopeptidase-like kinase chromatin-associated) transcription complex (Kisseleva-Romanova et al., 2006). Genetic and protein interaction analysis suggest the contribution of EKC in the control of transcription, translation and the cell cycle (Kisseleva-Romanova et al., 2006). In addition to Bud32, Kae1p, Cgi-121, Pcc2p and Pcc1p compose EKC. The composition of KEOPS and EKC are almost the same, with the exception of Pcc1p, a protein homologous to a human cancer-testis antigen, present only in EKC.

In humans, Bud32 homolog was originally isolated from activated cytotoxic T-cells and named PRPK (p53-related protein kinase), after functional assays uncovered its ability to phosphorylate p53 at Ser15. This result directly linked PRPK activity with p53 stabilization (Abe et al., 2001; Facchin et al., 2003). PRPK expression is detected in epithelial tumor cell lines, as well as in normal testis, showing a mild increase in G1 phase (Abe et al., 2001). In addition, human PRPK exhibits a predominantly cytoplasmic distribution and its activity is stimulated by Akt1 phosphorylation at Ser250 (Facchin et al., 2007).

Although the molecular nature of Bud32/PRPK has been documented in budding yeast and human cell lines, various unsettled issues remain regarding its functions. First, a p53 homolog

FONDAP Center for Genome Regulation, Departamento de Biología, Facultad de Ciencias, Universidad de Chile, Las Palmeras 3425, Santiago, Chile.

*Present address: Interdepartmental Biological Sciences Graduate Program, Northwestern University, Evanston, IL 60208, USA
‡Present address: Programa de Genética Humana, ICBM, Facultad de Medicina, Universidad de Chile, Independencia 1027, Santiago, Chile
§Author for correspondence (alglavic@uchile.cl)

Accepted 8 January 2013

has not been found in the *S. cerevisiae* genome. Thus, in humans, PRPK might be involved in an ancestral process other than regulating p53 stability. Second, Cgi-121, a component of KEOPS and EKC complexes, and interacting partner of PRPK (Miyoshi et al., 2003), is not present in the *Drosophila* genome. Finally, a completely different mechanism operates to control telomere dynamics in *Drosophila* (Purdy and Su, 2004; Cenci et al., 2005).

These reasons, together with the limited information about the physiological role of PRPK in metazoans, prompted us to examine the function of this ancestral kinase using the advantages of the fly model. Our results indicate that *Drosophila* PRPK is required for activation of the TOR kinase complex, being necessary autonomously for cell growth and proliferation, and therefore the control of body size.

MATERIALS AND METHODS

Drosophila melanogaster strains and phenotypic analysis

We used the following UAS lines: *UAS-CD8::GFP, UAS-Pi3K92E^{CAAX}, UAS-Akt1, UAS-S6K^{STDETE}, UAS-p35, UAS-foxo, UAS-RhebPA, UAS-p53^{DN}* (*UAS-p53^{R155H}*) (Ollmann et al., 2000); *UAS-p53, UAS-Rab5* (BDSC); *UAS-Tsc2i, UAS-Atg1i, UAS-p53i* (Vienna Drosophila RNAi Center, VDRC); and *UAS-RagA^{T16N}, UAS-RagA^{Q61L}, UAS-Rheb$^{EP50.084}$* (a gift from Dr Neufeld, Department of Genetics, Cell Biology and Development, University of Minnesota, Minneapolis, MN, USA). We also used the following Gal4 lines: *da-Gal4, cg-Gal4, ptc-Gal4, sal-Gal4 [sal^{EPv}-Gal4]* (Cruz et al., 2009); *nub-Gal4* (a gift from Dr de Celis, Centro de Biología Molecular Severo Ochoa, Madrid, Spain); and *tub-Gal4* (Bloomington Drosophila Stock Center, BDSC). The Prpk deficiency line used was Df(3L)GN24. Specific genetic descriptions are listed in supplementary material Table S1. All phenotypes were analyzed at 25°C unless stated otherwise, and wings were mounted for examination in lactic acid-ethanol (1:1). Pictures were taken in an Olympus MVX10 dissecting scope or Zeiss IIIRS microscope with a Leica DFC300FX digital camera and processed using Adobe Photoshop CS3 Extended.

UAS-Prpk constructs

Prpk-myc C-terminal fusion was constructed amplifying the coding sequence from genomic DNA using the primers: 5′-ATGTCCCTAG-AAATCCTGAAACAAGG-3′ and 5′-GCCTGAATTCACCAATCATG-GTTCTT-3′. The amplicon was cloned into the pGEMT-Easy vector (Promega) and sequenced. Afterwards it was subcloned into the pUAS-T-myc vector using *Eco*RI. A second UAS construct was developed to express a N-terminal FLAG version of Prpk (*FLAG-Prpk*); this was carried out using similar primers and cloned through Gateway technology (Invitrogen). Two RNAi constructs were made, with the complete Prpk sequence (675 bp) and with an internal fragment (462 bp). The internal fragment was amplified using the primers: 5′-CCCAGATCACGCGGCAGCGC-3′ and 5′-AGGCGGCCAGGACGTGCTCG-3′. The following cloning protocol was made for these constructs. PCR product was cloned into the pST Blue (Novagene) vector and sequenced. Next, it was subcloned using the *Sac*I and *Bam*HI sites in the pHIBS vector (Nagel et al., 2002). The *Not*I *Pst*I fragment from pST Blue Prpk and the *Pst*I *Xho*I fragment from pHIBS Prpk were directionally cloned in pBK SK *Not*I and *Xho*I sites to obtain the hairpin construct. Finally, the inverted repeat construct was introduced in the pUAS-T vector using the *Kpn*I and NotI sites. Mutant Prpk constructs were generated by site directed mutagenesis using the QuikChange kit (Stratagene) or directly by PCR using mutagenized primers, sequenced and cloned into pUAST. All primers and cloning strategies are summarized in supplementary material Table S2. A standard germ cell transformation was followed to obtain at least three independent transgenic insertions for each construct (Spradling and Rubin, 1982).

Immunofluorescence, western blot and RT-PCR analysis

Mouse monoclonal anti-BrdU (1/100, Hybridoma bank), anti-human PRPK [1/200, a gift from Dr Pinna, Department of Biological Chemistry and CNR Institute of Neurosciences, University of Padova, Padova, Italy (Facchin et al., 2007)] and anti-activated caspase 3 (1/100, Cell Signaling) were employed. Secondary antibodies were from Jackson Immunological Laboratories (1/200), nuclei were stained with Topro 3A (1/200, Invitrogen) and F-actin with TRITC-labeled phalloidin (1μg/ml, Sigma). Third instar imaginal discs were dissected, fixed and stained as described by de Celis (de Celis, 1997). Confocal images were captured using a Zeiss LSM 510 Meta confocal microscope.

For western blot, rabbit polyclonal PRPK (1/1000) (Facchin et al., 2007), phospho-S6K (1/500, Cell Signaling), S6K (1/500) (Montagne et al., 1999), phospho-4E-BP (1/500, Cell Signaling), rat polyclonal 4E-BP (1/1000), rabbit anti-myc (1/1000, Cell Signaling) and mouse anti-actin (1/5000, Santa Cruz Biotechnology) were used and the blotting was performed essentially as described previously (Hennig et al., 2006).

For RT-PCR, total RNA was extracted from embryos at stages 2, 7, 15 (Campos-Ortega and Hartenstein, 1985) and third instar larvae stage using Trizol reagent (Invitrogen). cDNAs were synthesized with the Improm-II kit (Promega). The following PCR protocols and primers were used. For *Prpk* expression: 25 cycles, annealing 55°C and elongation 45 seconds, primers used for the internal Prpk fragment were employed. For the 4E-BP semi-quantitative RT-PCR analysis: 30 cycles, annealing 55°C and elongation 45 seconds, forward primer 5′-CAACGGTGAACACATAGCAGCC-3′ and reverse 5′-CGAGAGAACAAACAAGGTGGAAGA-3′.

LysoTracker staining, BrdU and TR-avidin assays

Fat bodies were stained with LysoTracker as described previously (Scott et al., 2004). Larvae starvation was carried out in 0.8% agarose-PBS for 2 hours. BrdU incorporation was examined incubating carcasses in 0.05 mM BrdU in PBS for 20-30 minutes. Tissues were fixed in modified Carnoy's solution (3:1 ethanol: acetic acid) for 20 minutes, washed in PBS-0.3% Triton four times for 10 minutes each and DNA was hydrolyzed with 2 M HCl for 1 hour. After four washes in PBS/0.1% Tween, carcasses were incubated with anti-BrdU antibody (1/100). Later washes and secondary antibody incubation were carried out following standard immunofluorescence protocols. Endocytic assays using Texas Red-Avidin were performed following the protocol described previously (Hennig et al., 2006).

Flip-out clonal analysis

All the stocks employed were generated by standard crosses. Parental and specific experimental genotypes are described in supplementary material Table S1. Offspring was subjected to heat shock (37°C) at 36±12 or 60±12 hours after egg laying (AEL) for 2 minutes (fat body clones) or 7 minutes (imaginal tissue clones). Third instar larvae possessing clones (GFP positive) were processed and visualized by confocal microscopy. TR-avidin and autophagy assays were performed in 60±12 hours clones.

Statistical analysis

The estimation of larval volume was calculated, from at least 30 larvae, as a revolution ellipsoid with the formulae $4/3\pi\ ab^2$, with 'a' being the larval length and 'b' larval width. Wing hairs and distance between veins III and IV were quantified with the Photoshop Analysis tool from at least 30 samples, and depicted as a relative percentage to *sal>GFPnls* wings. Area quantification was performed from wing pouch clones and fat body cells using ImageJ software. All data presented are mean±s.d. and were subjected to Student's two-tailed *t*-test. *P* values lower than 0.01 were considered to be significant.

RESULTS

Drosophila Prpk

A BLAST search of the *Drosophila* proteome using human PRPK and yeast Bud32p sequences identifies CG10673-PA as the top hit ($E=10^{-52}$ and $E=10^{-28}$, respectively). Conversely, reciprocal BLASTing of human and yeast proteome with CG10673-PA identifies PRPK and Bud32p as establishing an orthology relationship. Genomic structure analysis predicts a single transcript with no introns that codes for a 224 amino acids Ser/Thr kinase (http://www.flybase.org/reports/FBgn0035590.html). RT-PCR reveals that *Prpk* is present from syncytial stage and is transcribed

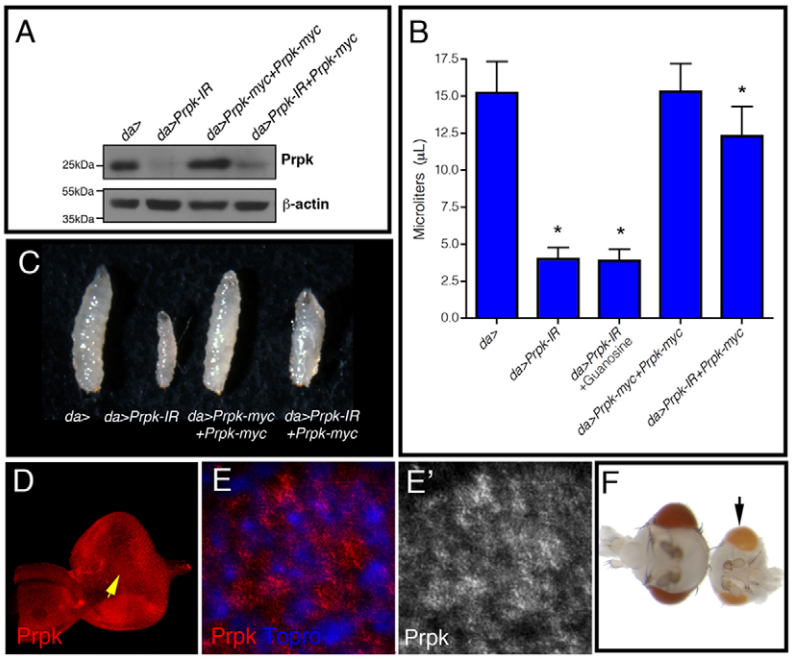

Fig. 1. Prpk expression and its requirement in animal growth. (**A**) Western blot analysis of Prpk levels of third instar larvae with generalized expression of the *Prpk-IR* and myc constructs. (**B**) The variations in larval volume between control (*da-Gal4*), knockdown (*da>Prpk-IR*), overexpressing larvae (*da>Prpk-myc*), rescued larvae (*da>Prpk-IR+Prpk-myc*) and Prpk-depleted larvae grown in 2 mg/ml guanosine-supplemented media ($n>30$ for each genotype). Data are mean±s.d. *$P<0.01$. (**C**) Representative cases of control (*da>*), knockdown (*da<Prpk-IR*), overexpressing (*da>Prpk-myc+Prpk-myc*) and rescued larvae (*da>Prpk-IR+Prpk-myc*). (**D**) *Prpk* is ubiquitously expressed in the antenna-eye disc with no obvious variations during the cell cycle or stage of differentiation (yellow arrow). (**E**,**E′**) Topro stain reveals the preferential cytoplasmic localization of Prpk. (**F**) Control (*nub-Gal4*) and Prpk knockdown (*da>Prpk-IR*, black arrow) pharate heads illustrating the strong reduction in body size without patterning or differentiation defects.

throughout the embryonic stage and at third instar larval stage (supplementary material Fig. S1).

To study *Prpk* function, we developed two activating hairpin constructs to target *Prpk* – both of them without predicted off-targets (defined as 19 nucleotides present in other places of *Drosophila* genome). Their efficiency was tested using an anti-human PRPK antibody (Facchin et al., 2007). Ubiquitous expression of these constructs produced a strong reduction in Prpk levels (Fig. 1A). This was similarly elicited by different insertions of both constructs and hereafter the results described were generated with an insertion of the internal hairpin RNA (462 bp; supplementary material Fig. S1).

Immunofluorescence analysis indicates that Prpk is expressed ubiquitously in imaginal discs. In eye discs, where cells in S and G2 phases can be recognized near the morphogenetic furrow (arrowhead, Fig. 1D), Prpk is expressed homogeneously throughout the cell cycle and in differentiating cells, locating preferentially at the cytoplasm of imaginal cells (Fig. 1E,E′). Interestingly, generalized knockdown of Prpk (*da>Prpk-IR*) produced a clear reduction in larval size (Fig. 1C). Although pupation was inhibited in Prpk-depleted larvae, some escapers did reach adulthood without patterning or differentiation defects, though size reduction remained (Fig. 1F). Prpk overexpression did not produce any recognizable phenotype, even though it was efficiently expressed (Fig. 1A-C), suggesting that it has a permissive rather than an instructive role in tissue growth.

A yeast two-hybrid assay has shown that Bud32 interacts with IMD (Inosine Monophosphate Dehydrogenase) proteins; thus, *Drosophila* Prpk might participate in guanosine synthesis (Lopreiato et al., 2004). Guanosine deficiency could explain the reduction in larval growth (guanosine auxotroph); however, *da>Prpk-IR* larvae grown in media supplemented with 2 mg/ml of guanosine, a treatment previously used to overcome guanosine deficiency in *Drosophila* (O'Donnell et al., 2000), did not recover the growth phenotype (Fig. 1B).

Prpk is required for cellular and organismal growth in *Drosophila*

Considering that size reductions were observed in larvae and in adults expressing *Prpk-IR*, it seemed possible that growth of larval and imaginal tissues was compromised. Indeed, expression of *Prpk-IR* in the salivary gland (*ptc-Gal4*, a driver not specific for salivary gland but with expression in this tissue) or in the fat body (*cg-Gal4*) markedly diminished their size (supplementary material Fig. S2). In addition, mosaic analysis showed that cell size reduction is cell-autonomous (Fig. 2G), indicating that Prpk is required in each larval cell. Importantly, this effect was reverted by the expression of *Prpk-myc* (Fig. 2J, quantified in 2K), showing the specificity of the Prpk knockdown phenotype.

As already mentioned, the reduction in adult size suggests that growth deficiencies are also produced in imaginal tissues; in this case, it could arise as a cause of decrease cell growth, proliferation or viability. To clarify this point, we analyzed the Prpk knockdown phenotype in the *Spalt* domain of adult wings (*sal-Gal4*, labeled green in Fig. 2A). A clear reduction in the distance between vein III and IV was produced (black line, Fig. 2A,E, quantified in Fig. 4). Consistently, imaginal discs expressing *Prpk-IR* displayed immunoreactivity to activated caspase 3, indicating apoptosis activation, particularly in proliferative cells (supplementary material Fig. S2). However, wing size could not be rescued by the expression of the anti-apoptotic protein p35 (Fig. 2L), suggesting that wing size phenotype was not exclusively caused by apoptosis induction.

In accordance with the cell death induced in the wing disc, we observed that viability of Prpk-deficient clones was also reduced. Early Prpk-depleted clones (36±12 hours AEL) were not found in third instar wing discs. However, clones induced later (60±12 hours AEL) were disaggregated and showed apoptotic features (Fig. 2F). By contrast, clones co-expressing p35 and *Prpk-IR* were found, not disaggregated, although their size was reduced (Fig. 2M). BrdU incorporation in these clones showed that cells proliferate more slowly (Fig. 2N). Together, clone size reduction and BrdU assay suggest that tissue size reduction could be, at least in part, the result of fewer cells present in Prpk knockdown tissues.

Finally, to evaluate whether *Prpk* knockdown also impairs imaginal cell growth, we estimated cell density in adult wings by quantifying the number of hairs (each cell produces one) present in a defined area within the *Spalt* domain (red square, Fig. 3A). This parameter illustrates that *Prpk* knockdown decreases cell size (Fig. 3B,C,

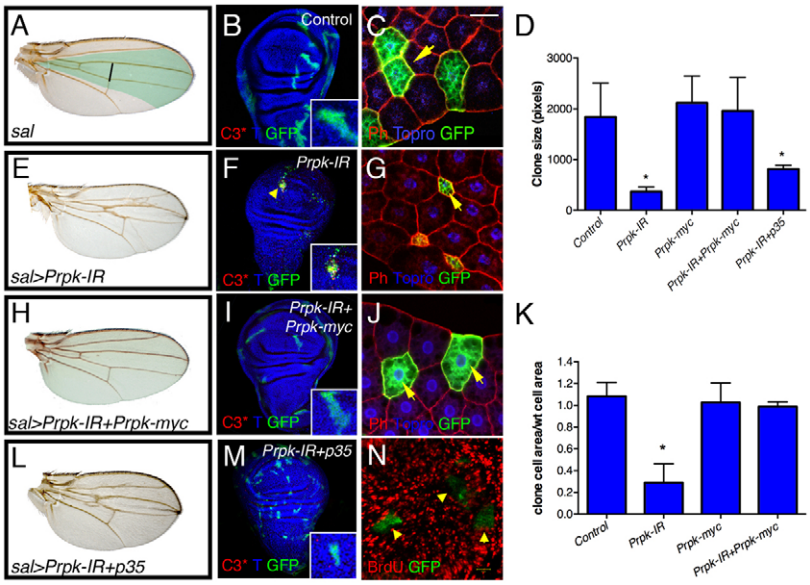

Fig. 2. Prpk is necessary for imaginal tissue proliferation and larval cell growth. (**A**,**E**,**H**,**L**) Female adult wings. (A) Control wing showing the *Spalt* domain (green area, *sal=sal-Gal4*). Expression of *Prpk-IR* (E, *sal>Prpk-IR*) reduces wing size even in the presence of the apoptosis inhibitor p35 (L, *sal>Prpk-IR+p35*). The reduction in organ size is reverted by *Prpk-myc* co-expression (H, *sal>Prpk-IR+Prpk-myc*). (**B**,**F**,**I**,**M**,**N**) Wing imaginal disc with clones induced at 60±12 hours AEL (GFP-positive cells), stained with Topro (T, blue) and activated caspase 3 (C3*, red). Mosaic control wing disc (B). Prpk knockdown clones are small and apoptotic (F, arrowhead). This is rescued by co-expressing *Prpk-myc* (I). (M,N) Prpk-deficient clones expressing the apoptosis inhibitor p35. Clones appear without apoptotic features but are small and incorporate less BrdU (N, arrowheads, clones induced at 35±12 hours AEL). (**C**,**G**,**J**) Fat body clones induced at 36±12 hours AEL stained with Topro (blue) and phalloidin-TRITC (red). Control clones (GFP, arrow) grow normally (C). Conversely, *Prpk-IR* inhibits growth in a cell-autonomous manner (G, arrow) and this is also alleviated by increasing Prpk levels (J). Scale bar: 50 μm in C,G,J; 10 μm in N. (**D**) Imaginal clone size of the genotypes described on the *x*-axis. Ten imaginal discs and at least 20 clones were analyzed for each genotype. (**K**) Clonal cell area relative to wild-type neighbor cells in fat body. At least 25 experimental clones and 30 neighbor cells were quantified. Data are mean±s.d. **P*<0.001.

quantified in 3I) and, similar to tissue size reduction, this is not prevented by apoptosis inhibition (Fig. 3E,I). Interestingly, growth phenotypes were completely reverted by Prpk overexpression, but this reversion was only partial with a kinase-dead form of Prpk (Fig. 3G,I; supplementary material Fig. S4), indicating a residual kinase activity for this mutant or a main structural role for this kinase in cell growth. These observations are similar to those described in yeast (Lopriato et al., 2004; Peggion et al., 2008; Srinivasan et al., 2011). Together, these data suggest that Prpk is a component of the growth-promoting machinery that allows cell-mass accumulation in larval tissues, as well as cell growth, proliferation and viability in imaginal discs.

Reductions in tissue size produced by Prpk knockdown are independent of p53

Human PRPK has been associated with p53 stabilization owing to its ability to phosphorylate it at Ser15 (Abe et al., 2001; Facchin et al., 2003). In *Drosophila*, p53 controls the cell cycle and apoptosis under genotoxic conditions (Ollmann et al., 2000). In view of this, we asked whether this phosphorylation site is conserved in *Drosophila* p53 and whether it is related with the wing phenotype observed. In silico examination of p53 isoforms showed that two of them have putative phosphorylation sites at Ser13 and Ser16 (NetPhos 2.0 Server; supplementary material Fig. S3). Next, we tested whether modifying Prpk levels could alter the wing phenotype caused by mild overexpression of p53. Co-expression of p53 with *Prpk-IR* caused an increment of this phenotype in disagreement with the expected reduction of stabilized p53. In addition, co-expressing *Prpk-IR* with a dominant-negative form of p53 or with *p53-RNAi* does not modify the *Prpk-IR* wing phenotype (supplementary material Fig. S3). These results reveal that Prpk knockdown wing phenotype does not depend on p53 levels.

Prpk is required for PI3K/TOR-induced cell growth and for proliferation in larval and imaginal tissues

Activation of PRPK and Bud32 is controlled by Akt1 in human cell lines and Sch9 in yeast (Facchin et al., 2007; Peggion et al., 2008). The Akt phosphorylation motif R-x-R-x-x-p(S/T) is conserved in human, fly and yeast Bud32/PRPK proteins (supplementary material Fig. S4). Therefore, and considering the growth phenotype of Prpk knockdown animals, we studied the possibility that Prpk activity might be regulated by Akt1 and by part of the PI3K and/or TOR signaling pathways, both major contributors in the regulation of cell growth in *Drosophila* and mammalian cells (Kozma and Thomas, 2002; Oldham and Hafen, 2003).

We generated UAS constructs to express forms of Prpk with mutated Akt1 phosphorylation sites in the wing disc in order to test their abilities to modify tissue growth and to suppress the Prpk knockdown phenotype (supplementary material Fig. S4). Neither the phospho-mimetic mutants ($Prpk^{T221D}$ or $Prpk^{T221E}$) nor Prpk lacking the Akt1 phosphorylation site ($Prpk^{T221A}$) affected wing size; however, both mutants were effective suppressing the cell growth wing size phenotype produced by *Prpk-IR*.

Following our reasoning, we analyzed the role of Prpk in PI3K/TOR pathways. First, as a readout of PI3K activation, we tested whether reducing Prpk levels could change the amount of PIP3 at the plasma membrane (Britton et al., 2002). No changes in the distribution of pleckstrin-homology domain GFP fusion protein were observed in Prpk knockdown animals (supplementary material Fig. S5).

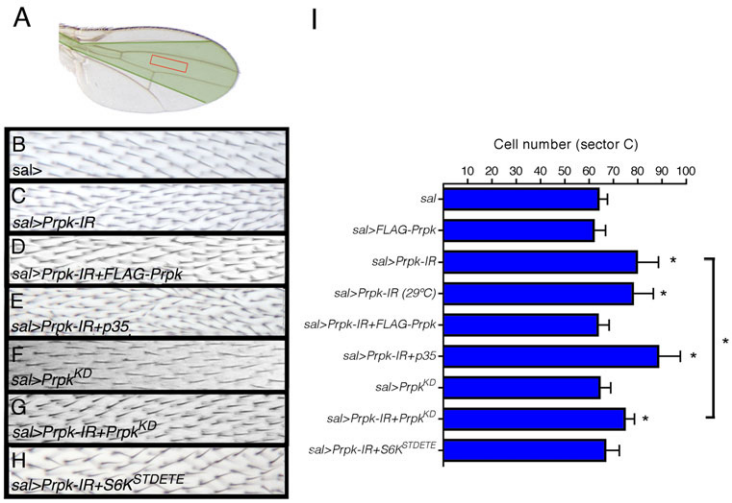

Fig. 3. Wing cell growth requires Prpk function. (**A**) Wild-type female wing indicating the area (outlined) used for cell number quantification. (**B-H**) Wing hair patterns obtained in each condition. (B) Control wing (*sal-Gal4*). (C) Prpk-depleted wing (*sal>Prpk-IR*). (F) Kinase-dead mutant (*sal>Prpk^{KD}*). Overexpression of Prpk (D, *sal>Prpk-IR+FLAG-Prpk*) or its kinase-dead mutant (G, *sal>Prpk-IR+Prpk^{KD}*) completely and partially reverts cell growth deficiency. (E) Apoptosis inhibition by p35 expression in Prpk-depleted wing (*sal>Prpk-IR+p35*) does not prevent the cell size phenotype. (H) Co-expression of *Prpk-IR* with an activated form of S6 kinase (*sal>Prpk-IR+S6K^{STDETE}*) abolished cell size reduction (compare H with C). (**I**) Cell number quantifications. Quantification was performed by counting the number of hairs in a minimum of 15 female wings for each condition (*P<0.001). Data are mean±s.d.

Then, we tested whether positive regulators of PI3K and TOR could counteract the effects of lessening Prpk in adult wings and larval tissues. The wing size reduction produced by decreasing Prpk function was not abolished by its co-expression with an activated PI3K subunit (Fig. 4J,S), Akt1 (Fig. 4L,S), Tsc2-RNAi (Fig. 4S; supplementary material Fig. S3) or Rheb (Fig. 4N,S). Conversely, co-expression with an activated form of S6K (S6K^{STDETE}) (Barcelo and Stewart, 2002) completely abolished the wing growth deficiency (Fig. 4P,S), suggesting that *Prpk* could be a downstream or a parallel component of the TOR pathway required for its growth-promoting activity. When using *sal-Gal4*, no apparent wing size phenotype was produced by these constructs (Fig. 4I,K,M,O, quantified in 4S). In accordance with wing size recovery, co-expression of *Prpk-IR* with the activated form of S6K was also efficient in restoring cell growth (Fig. 3H,I). Thus, these functional interactions indicate that, with respect to adult wing and to cell sizes, Prpk acts downstream or in parallel with Rheb, and upstream of S6K activation. Additionally, we tested whether Prpk overexpression could modify the outcome produced using the *sal-Gal4* driver to change PI3K/TOR signaling in the developing wing disc. No obvious effects were detected under these circumstances (supplementary material Fig. S6).

We performed mosaic analysis to establish whether the relationships between Prpk and the PI3K/TOR pathway, described for adult wing, works cell-autonomously in imaginal and larval cells. First, we analyzed whether normal growth rates could be

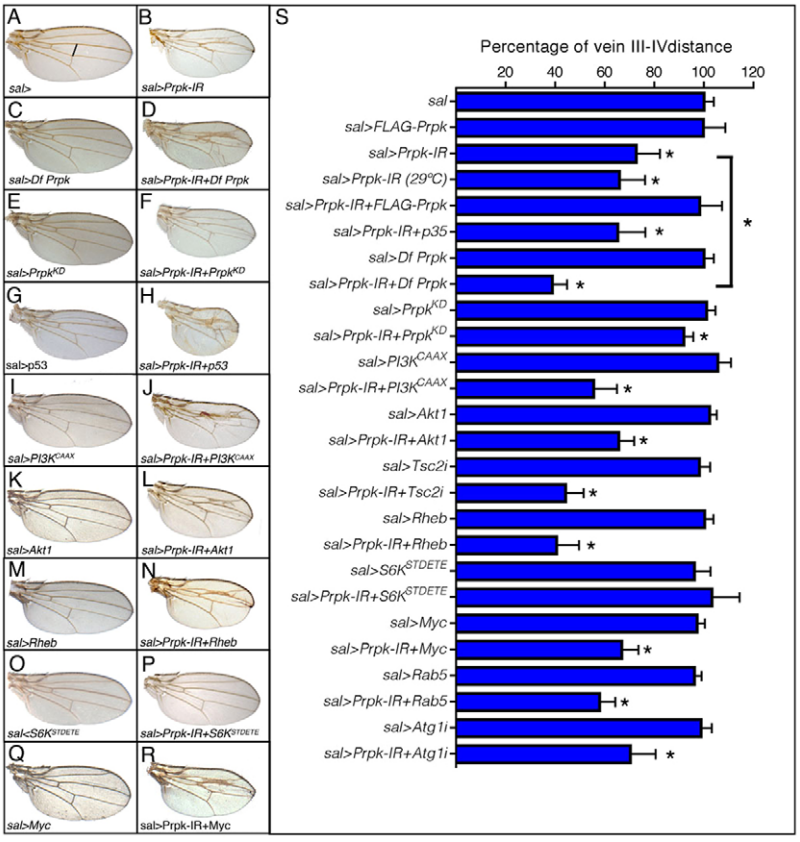

Fig. 4. PI3K/TOR-dependent cell growth and proliferation require Prpk function to sustain adult size. (**A-R**) Female adult wings expressing the indicated constructs in the central pouch. Prpk depletion reduces wing size (B, *sal>Prpk-IR*). This is enhanced by expressing it in a deficiency background covering the *Prpk* locus (D, *sal>Prpk-IR/Df(3L)GN24*). A Prpk kinase-dead mutant partially rescues the wing phenotype (F, *sal>Prpk-IR+Prpk^{KD}*). *Prpk-IR* reduces wing size in presence of p53 (H, *sal>Prpk-IR+p53)*. The reduction in wing size is not reverted by co-expression with an activated form of PI3K (J, *sal>Prpk-IR+PI3K^{CAAX}*), Akt1 (L, *sal>Prpk-IR+Akt1*) or Rheb (N, *sal>Prpk-IR+Rheb*). Conversely, co-expression of *Prpk-IR* with an activated form of S6 kinase suppresses the phenotype (P, *sal>Prpk-IR+S6K^{STDETE}*). Myc expression did not rescue the *Prpk-IR* phenotype (R, *sal>Prpk-IR+Myc*). (**S**) Wing size reduction as a percentage of the distance between veins III and IV (black line in A). Quantification was performed by measuring the distance between veins in a minimum of 30 female wings for each condition and the resulting average standardized to control value (*sal-Gal4*) (*P<0.001). Data are mean±s.d.

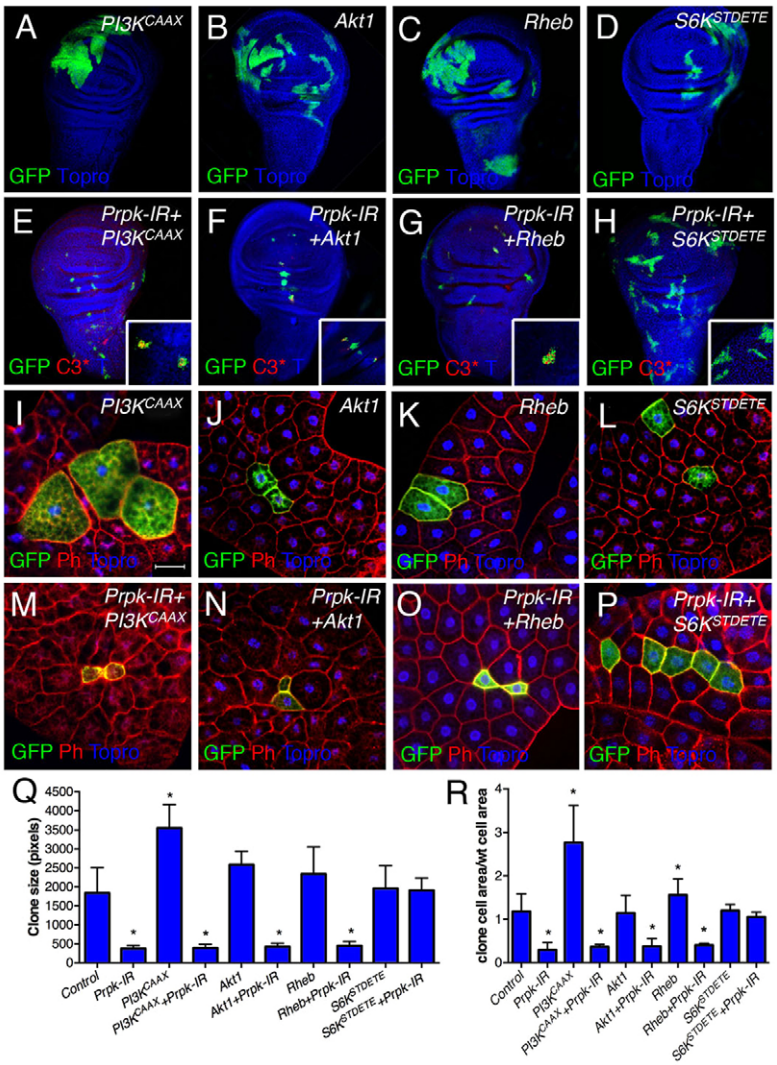

Fig. 5. Clonal analysis of Prpk function and its hierarchical relationship with components of the PI3K/TOR pathway. (**A-H**) Wing discs with clones, induced at 60±12 hours AEL, expressing the indicated constructs (GFP cells), stained with Topro (blue) and activated caspase 3 (C3*, red). Scale bar: 110 μm. (A) Clones expressing the activated PI3K form (*UAS-PI3K^{CAAX}*) proliferate extensively and no caspase 3 activation is detected. (E) Prpk reduction inhibits the growth-promoting activity of PI3K^{CAAX}, thus clones grow poorly and are apoptotic (inset). (B,C) Normal growth is observed in Akt1 and Rheb-overexpressing clones. However, *Akt-* or *Rheb-Prpk-IR* clones are also small and apoptotic (inset) (F,G). (D) Clones expressing the activated form of S6K (*UAS-S6K^{STDETE}*) proliferate normally with no evidence of apoptosis (D). (H) *S6K^{STDETE}-Prpk-IR* clones proliferate normally and no apoptosis is detected (inset). (**I-P**) Fat bodies with clones induced at 36±12 hours AEL expressing the indicated constructs (GFP cells), stained with Topro (blue) and phalloidin-TRITC (red). Scale bar: 50 μm. (I) PI3K-overexpressing cells grow to exceed the size of surrounding control cells. (M) Co-expression of *Prpk-IR* with *PI3K^{CAAX}* completely inhibits this overgrowth. (J,K) No significant or mild increase in size was detected in cells expressing Akt1 (J) and Rheb (K). (N,O) A clear reduction in cell size is detected in clones expressing *Prpk-IR* with Akt1 or Rheb. (L) Clones expressing the activated S6K form grow in the same way as surrounding cells. (P) *S6K^{STDETE}-Prpk-IR* clones grow as much as surrounding wild-type cells. (**Q**) Wing disc clonal area (*P<0.001). (**R**) Cell size in fat body clones. Quantifications were performed by counting the clones or measuring the area in a minimum of 10 discs and over 20 clones for each condition. Area of fat body clonal cells was normalized with the average area of surrounding control cell (*P<0.001). Data are mean±s.d.

rescued in Prpk-depleted clones expressing components of the PI3K/TOR pathway. Activated PI3K, Akt or Rheb-expressing clones grew as expected (Fig. 5A-C); however, clones co-expressing each of these constructs with *Prpk-IR* were apoptotic and small (Fig. 5E-G and insets, quantified in 5Q). Conversely, a clear rescue in clone growth was detected in clones co-expressing the activated form of S6K and *Prpk-IR* (Fig. 5H and inset). These results support our previous data and imply that Prpk is required cell-autonomously in proliferating tissues to translate the PI3K/TOR growth input into the protein biosynthetic capacity that regulates S6K activity.

Like imaginal discs, larval tissues grow in response to insulin and TOR activities. However, larval tissues support their growth by mass accumulation. Through a similar mosaic strategy, we investigated whether the relationship between the PI3K/TOR pathway and Prpk also operates in these non-proliferating cells. Activated PI3K clones in the fat body grew extensively without obvious non-autonomous effects (Fig. 5I,R). This was obliterated by Prpk depletion (Fig. 5M). Similarly, Akt1 or Rheb expression was insufficient to allow cell growth under Prpk depletion (Fig. 5N,O, quantified in 5R). Conversely, cell size phenotype was entirely reverted by the expression of the S6K activated form (Fig. 5P). These analyses demonstrate that Prpk is required cell-autonomously to sustain larval cell growth and, equivalent to what is observed in proliferating cells, appears to be essential to translate PI3K/TOR signal to S6K activation.

Amino acids, through Rag A and C GTPases, can shift TOR from the cytoplasm towards late endosomes, where it can interact with Rheb (Sancak et al., 2008; Kim et al., 2008; Sancak et al., 2010). Overexpression of a dominant-negative or constitutive version of RagA (RagA^{T16N} and RagA^{Q61L}) (Kim et al., 2008) with *Prpk-IR* did not change Prpk knockdown wing phenotype (supplementary material Fig. S3), suggesting that TOR activation by RagA was not affected. A parallel network also related with protein translation, cell growth and proliferation is controlled by Myc (reviewed by Gallant, 2009). To determine whether Prpk is also connected to this network, we tested whether the co-expression of Myc and *Prpk-IR* could revert adult wing size. As expected from Prpk requirement in S6K activation, Myc was unable to rescue wing size (Fig. 4R).

Prpk is essential for the phosphorylation of TOR kinase targets

TOR kinase is the primary activator of S6K, phosphorylating Thr398 to allow Thr422 phosphorylation by PDK1 (Isotani et al., 1999). Among the regulatory interactions that control cell growth and proliferation, besides S6K, TOR also phosphorylates 4E-BP, inhibits macroautophagy and stimulates endocytosis (Edgar, 2006).

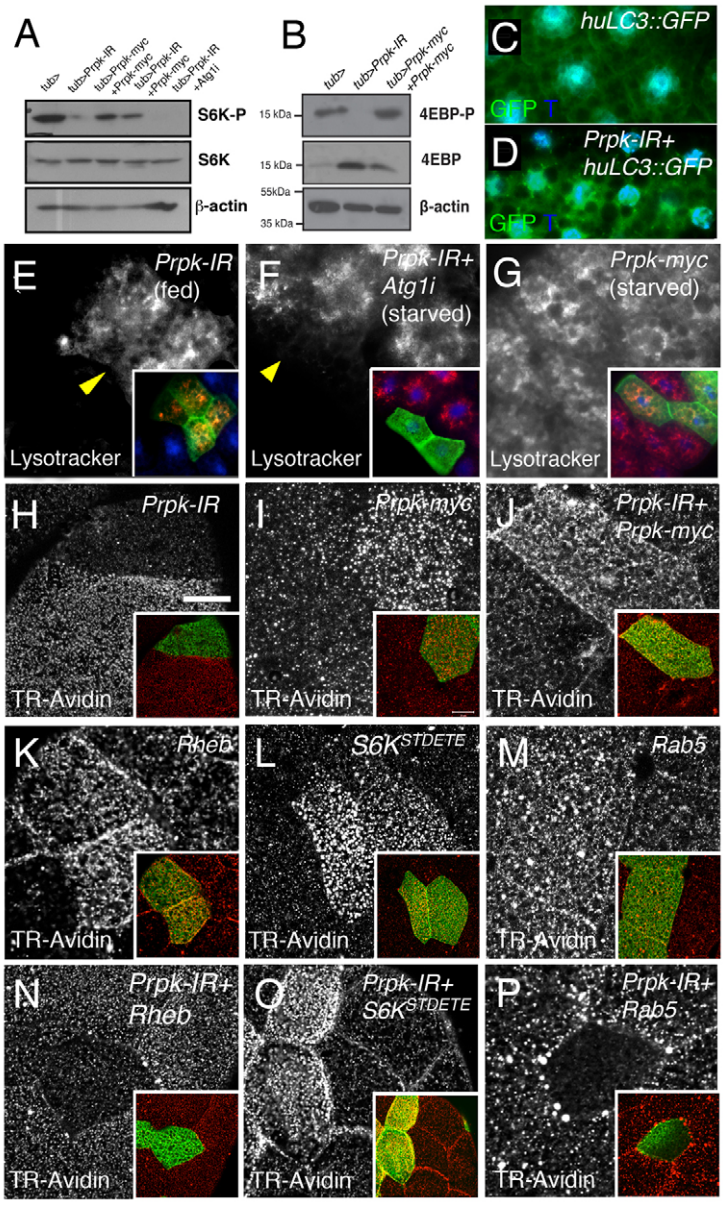

Fig. 6. Prpk is essential for the regulation of TOR targets: S6K and 4EBP phosphorylation, autophagy and endocytosis. (**A**,**B**) Western blot analysis of S6K and 4E-BP phosphorylation mediated by TOR in larvae expressing different Prpk levels. (**C**,**D**) Fat bodies expressing the autophagy marker LC3::GFP in control (C, *da >huLC3::GFP*) and *Prpk-IR* (D, *da >huLC3::GFP+Prpk-IR*) animals. Autophagosome appearance (GFP-positive vesicles) reveals autophagy induction (**E**) Fat body Prpk-knockdown clones of fed larvae are positive for LysoTracker stain (arrowhead). (**F**) Atg1 depletion blocks autophagy induction in Prpk knockdown clones of starved larvae (arrowhead). (**G**) Autophagy is not prevented by Prpk overexpression in starved larvae (*da>Prpk-IR*). (**H-P**) Bulk endocytosis assays. (H) Fat body Prpk-deficient clones incorporate TR-avidin inefficiently. (I-K) Prpk overexpression (I) and *Prpk-IR* co-expression (J) or Rheb co-expression (K) increase clone endocytosis. (L,O) $S6K^{STDETE}$ (L) also increases endocytosis and its co-expression with *Prpk-IR* (O) is capable of rescuing clone endocytosis. (N) Rheb overexpression in fat body clones depleted of Prpk is not able to rescue the endocytic blockage. (M,R) Rab5 overexpression also increases clone endocytosis (M), but is incapable of recovering TR-avidin uptake when is expressed together with *Prpk-IR* (P). Scale bar: 30 μm.

Western blot analysis confirmed that Prpk is essential for TOR phosphorylation of S6K and 4E-BP (Fig. 6A,B), showing that Prpk is either necessary for TORC1 activation or for its functional interaction with both targets.

Fasting or reduced PI3K/TOR activity induce macroautophagy in *Drosophila* (Scott et al., 2004; Rusten et al., 2004; Kim et al., 2008; Meléndez and Neufeld, 2008). In accordance with the attenuation of TOR activity, fat body *Prpk*-depleted cells were positive for LysoTracker stain (Fig. 6E) and autophagosome vesicles (huLC3::GFP positive punctae) (Fig. 6C,D), suggesting macroautophagy induction. Atg1 mediates macroautophagy induction and additionally inhibits S6K phosphorylation (Lee et al., 2007; Scott et al., 2007). To rule out diminished S6K phosphorylation as the cause of this, we simultaneously knocked down Atg1 and Prpk in fat body cells. As expected, this procedure efficiently impeded macroautophagy induction under starvation (Fig. 6F), but was unable to prevent the reduction in S6K phosphorylation (Fig. 6A) or the Prpk knockdown wing phenotype (supplementary material Fig. S3P, quantified in S3S).

A previous report has shown a bi-directional association between endocytosis and TOR activation. Thus, increasing TOR activity rises bulk endocytosis, while altering endocytosis in ATPase Hsc70-4 mutant cells represses it (Hennig et al., 2006). To further extend the analysis to other targets of TOR, we asked whether Prpk depletion could also modify endocytosis. Clonal analysis in the fat body reveals that Prpk knockdown blocked bulk endocytosis (Fig. 6H). By contrast, the increase in Prpk or the co-expression of *Prpk-IR* with *Prpk-myc* enhances Texas Red-avidin uptake (Fig. 6I,J). To determine whether Prpk regulates endocytosis directly (explaining TOR inhibition) or through its effects on TOR itself, we directly activated endocytosis overexpressing Rab5 alone or together with *Prpk-IR*. Rab5 overexpression caused an increase in endocytosis; however, this was prevented when Prpk was reduced (Fig. 6M,P). Similarly, activation of endocytosis was insufficient to recover the wing phenotype (supplementary material Fig. S3R).

Together, these results show that Prpk is fundamental in the regulation of TOR kinase activity and, therefore, the

phosphorylation of S6K and 4E-BP, autophagy repression and endocytosis control. Although Prpk gain of function enhanced endocytosis in the fat body (Fig. 6I), it was unable to suppress autophagy induction during starvation (Fig. 6G) or increase S6K and 4E-BP phosphorylation (Fig. 6A,B), further suggesting the permissive character of Prpk in TOR activation.

DISCUSSION

In this study, we have analyzed the role of p53-related protein kinase (PRPK) in an animal model system. Our results show that *Drosophila* PRPK (*Prpk*) is necessary for TOR activation and for the translation of PI3K/TOR growth signals to their targets, which lastly support cell growth and proliferation to sustain organ and body growth.

Prpk is required to sustain organ growth to attain final body size

Analogous to what has been observed in animals with mutations in positive components of PI3K/TOR pathway, diminishing Prpk function reduces organ and body size without major patterning or differentiation defects. As *Prpk* alleles are not available, we developed a RNA interference strategy to address its function. Although our *Prpk-IR* constructs are efficient at silencing Prpk, they cause hypomorph conditions. Hence, the wing phenotype produced by *Prpk-IR* was enhanced by removing one copy of the *Prpk* locus [Df(3L)GN24]. It is important to note that *Prpk-IR* phenotypes are reverted by Prpk co-expression, showing their specificity. Interestingly, a kinase-dead form of Prpk or different Akt1 phosphorylation mutants also produced this reversion, suggesting a structural, Akt1 independent, role for this kinase in tissue growth. This is analogous to what has been described in yeast (Peggion et al., 2008).

The size reduction of Prpk-deficient larvae and adults suggests that growth defects occur in larval and imaginal tissues. Importantly, the growth phenotype in larval tissue is cell-autonomous, ruling out indirect effects due to alterations in the larval nutrient sensor mechanism (Colombani et al., 2003). This phenotype could be explained using data from a yeast two-hybrid assay, which shows that Bud32 interacts with IMD proteins and with glutaredoxin (Grx4) (Lopreiato et al., 2004), which suggests a role for Bud32 in nucleoside biosynthesis and REDOX balance. However, Prpk-depleted larvae fed with guanosine did not recover their normal size and no obvious REDOX variations were detected using the dihydro-dichloro-fluorescein di-acetate probe in Prpk-depleted clones (data not shown), arguing against either possibility.

The precursors of the fly body grow mainly by proliferation, and analysis of Prpk knockdown in adult wing reveals that growth of its progenitors is diminished. Apoptosis inhibition shows that it has a negligible role in the reduction of organ size. Interestingly, analysis in apoptosis-inhibited knockdown wings indicates impaired cell growth. In addition, apoptosis-inhibited Prpk-deficient clones in the wing imaginal disc are smaller and show less BrdU incorporation, suggesting poor proliferation. This, together with cell size reduction, contributes to the final decrease in tissue size.

It has been shown that Bud32/PRPK can phosphorylate and stabilize p53, and this has been proposed to be a key target in human cells (Abe et al., 2001; Facchin et al., 2007). Under normal conditions, the lack of p53 in *Drosophila* has no influence on proliferation or cell survival, whereas its overexpression stimulates apoptosis (Ollmann et al., 2000). Thus, p53 stabilization should occur in Prpk-overexpressing imaginal cells thus eliciting apoptosis. Nevertheless, our results show and support the notion that Prpk depletion induces apoptosis independently of p53.

Prpk is essential for translating PI3K/TOR growth signals into cell proliferation and cell growth

Using the Prpk knockdown wing phenotype, we analyzed its functional interactions with PI3K, Akt1, Tsc2, Rheb and S6K, among others. Only the expression of an activated form of S6K was able to rescue the *Prpk-IR* phenotypes. In addition, clonal analysis established that Prpk/PI3K/TOR functional relationship operates cell-autonomously in larval and imaginal tissues. The S6K construct employed (*UAS-S6K^{STDETE}*) has activating substitutions at Ser418 and Thr422 in the autoinhibitory domain, and at Thr398 in the linker domain (Dennis et al., 1996; Pullen and Thomas, 1997). TOR has been implicated in this last phosphorylation (Isotani et al., 1999). Western blot analysis for this phosphorylation and the ability of the activated S6K form to overcome Prpk depletion further strengthens the idea that Prpk regulates cell growth and proliferation by modulating S6K activation in a TOR-dependent manner.

We found few and small Prpk-depleted clones in proliferating domains of imaginal discs, as well as caspase 3 activation within them. Thus, Prpk is necessary for the survival of proliferating imaginal cells. Interestingly, apoptosis is not exhibited in S6K mutant animals, where the reduction in tissue size is caused mostly by decreased cell size (Montagne et al., 1999), indicating that Prpk controls an element or elements required for TOR-mediated S6K activation, but with additional functions in cell survival. However, these requirements are concealed by activated S6K co-expression.

Prpk is involved in TOR activation

Several lines of evidence suggest that S6K activation is not the only process altered by Prpk knockdown; 4E-BP phosphorylation, autophagy, endocytosis and apoptosis were also distorted in these animals. These defects are similar to TOR loss-of-function phenotypes (Oldham et al., 2000; Zhang et al., 2000; Scott et al., 2007), suggesting that the main effect of Prpk depletion is the failure of TOR activation or it interaction with its targets, which ultimately impacts on cell viability, cell growth and proliferation.

High-throughput RNAi screening has identified S6K and TOR as activating elements for endocytosis in humans (Pelkmans et al., 2005). This strategy also identified PRPK (NM_33550), but it has milder effects, particularly on clathrin-mediated endocytosis. These observations could imply that Prpk is directly involved in the control of endocytosis, thus Prpk knockdown would decrease endocytosis and as a consequence TOR would be improperly activated. Although Prpk overexpression enhances bulk endocytosis in the fat body, we were unable to observe cell growth phenotypes, suppression of autophagy or an increase in the phosphorylation of S6K or 4EBP. Furthermore, the activated form of S6K effectively prevents the endocytic blockage generated by Prpk depletion. Therefore, we favor the scenario where Prpk is required as a permissive element for TOR and S6K activation, which indirectly modifies endocytosis. Perhaps the enhancement of endocytosis induced by Prpk overexpression is due to its stimulatory effects on TOR or S6K activation that our western blot and autophagy assays were insufficiently sensitive to reveal, or Prpk could have a more direct role in endocytosis that is shared by S6 kinase.

How can we reconcile our observations with what is known about Bud32/PRPK? Recently, EKC/KEOPS component mutants have been described as defective for N6-threonylcarbamoyl adenosine modification of tRNAs that decode ANN codons. This modification

modulates tRNA stability and affinity within ribosomes during anticodon recognition (El Yacoubi et al., 2011; Srinivasan et al., 2011), affecting ATG codon selection (Daugeron et al., 2011). We presume that Prpk depletion could affect this process and, through an unknown mechanism, decrease TOR activity and finally reduce protein synthesis. This could explain why Rheb overexpression or Tsc2 knockdown could not rescue Prpk reduction-of-function phenotypes; this is similar to what happen in after knockdown of Brf, which has been shown to be required for RNA polymerase III activity and for tRNA transcription (Marshall et al., 2012). Nevertheless, this hypothesis does not explain why S6K is capable of reverting *Prpk-IR* phenotypes. All the targets of S6K are probably not known; however, it is accepted that it can affect endocytosis (Hennig et al., 2006), autophagy (Scott et al., 2004) and even tRNA levels in cells (Marshall et al., 2012), so perhaps it could be also related with efficient start codon selection. Future studies with components of the EKC/KEOPS complex and S6K would reveal their function in codon selection and how this relates to TOR activity.

Acknowledgements
We thank Dr Pinna for kindly provide the PRPK antibody, Dr Neufeld, Dr Teleman and Dr de Celis for flies and antibodies. Additionally, we thank Marek Mlodzik and Miguel Allende for critical reading during the preparation of this manuscript, and the BDSC, VDRC and Hybridoma Bank for reagents.

Funding
This work was funded by Fondo de Financiamiento de Centros de Excelencia en Investigación (FONDAP) [15090007] and Fondo Nacional de Desarrollo Científico y Tecnológico (FONDECYT) [1100366] to A.G., and a Comisión Nacional de Investigación Científica y Tecnológica (CONICYT) PhD Fellowship to C.I.

Competing interests statement
The authors declare no competing financial interests.

Supplementary material
Supplementary material available online at
http://dev.biologists.org/lookup/suppl/doi:10.1242/dev.086918/-/DC1

References

Abe, Y., Matsumoto, S., Wei, S., Nezu, K., Miyoshi, A., Kito, K., Ueda, N., Shigemoto, K., Hitsumoto, Y., Nikawa, J. et al. (2001). Cloning and characterization of a p53-related protein kinase expressed in interleukin-2-activated cytotoxic T-cells, epithelial tumor cell lines, and the testes. *J. Biol. Chem.* **276**, 44003-44011.
Barcelo, H. and Stewart, M. J. (2002). Altering Drosophila S6 kinase activity is consistent with a role for S6 kinase in growth. *Genesis* **34**, 83-85.
Britton, J. S., Lockwood, W. K., Li, L., Cohen, S. M. and Edgar, B. A. (2002). Drosophila's insulin/PI3-kinase pathway coordinates cellular metabolism with nutritional conditions. *Dev. Cell* **2**, 239-249.
Campos-Ortega, J. A. and Hartenstein, V. (1985). *The Embryonic Development of Drosophila melanogaster*. Berlin: Springer-Verlag.
Cenci, G., Ciapponi, L. and Gatti, M. (2005). The mechanism of telomere protection: a comparison between Drosophila and humans. *Chromosoma* **114**, 135-145.
Colombani, J., Raisin, S., Pantalacci, S., Radimerski, T., Montagne, J. and Léopold, P. (2003). A nutrient sensor mechanism controls Drosophila growth. *Cell* **114**, 739-749.
Cruz, C., Glavic, A., Casado, M. and de Celis, J. F. (2009). A gain-of-function screen identifying genes required for growth and pattern formation of the Drosophila melanogaster wing. *Genetics* **183**, 1005-1026.
Danial, N. N. and Korsmeyer, S. J. (2004). Cell death: critical control points. *Cell* **116**, 205-219.
Daugeron, M. C., Lenstra, T. L., Frizzarin, M., El Yacoubi, B., Liu, X., Baudin-Baillieu, A., Lijnzaad, P., Decourty, L., Saveanu, C., Jacquier, A. et al. (2011). Gcn4 misregulation reveals a direct role for the evolutionary conserved EKC/KEOPS in the t6A modification of tRNAs. *Nucleic Acids Res.* **39**, 6148-6160.
de Celis, J. F. (1997). Expression and function of decapentaplegic and thick veins during the differentiation of the veins in the Drosophila wing. *Development* **124**, 1007-1018.
Dennis, P. B., Pullen, N., Kozma, S. C. and Thomas, G. (1996). The principal rapamycin-sensitive p70(s6k) phosphorylation sites, T-229 and T-389, are differentially regulated by rapamycin-insensitive kinase kinases. *Mol. Cell. Biol.* **16**, 6242-6251.
Downey, M., Houlsworth, R., Maringele, L., Rollie, A., Brehme, M., Galicia, S., Guillard, S., Partington, M., Zubko, M. K., Krogan, N. J. et al. (2006). A genome-wide screen identifies the evolutionarily conserved KEOPS complex as a telomere regulator. *Cell* **124**, 1155-1168.
Dufner, A. and Thomas, G. (1999). Ribosomal S6 kinase signaling and the control of translation. *Exp. Cell Res.* **253**, 100-109.
Edgar, B. A. (2006). How flies get their size: genetics meets physiology. *Nat. Rev. Genet.* **7**, 907-916.
Efstratiadis, A. (1998). Genetics of mouse growth. *Int. J. Dev. Biol.* **42**, 955-976.
El Yacoubi, B., Hatin, I., Deutsch, C., Kahveci, T., Rousset, J.-P., Iwata-Reuyl, D., Murzin, A. G. and de Crécy-Lagard, V. (2011). A role for the universal Kae1/Qri7/YgjD (COG0533) family in tRNA modification. *EMBO J.* **30**, 882-893.
Facchin, S., Lopreiato, R., Stocchetto, S., Arrigoni, G., Cesaro, L., Marin, O., Carignani, G. and Pinna, L. A. (2002a). Structure-function analysis of yeast piD261/Bud32, an atypical protein kinase essential for normal cell life. *Biochem. J.* **364**, 457-463.
Facchin, S., Sarno, S., Marin, O., Lopreiato, R., Sartori, G. and Pinna, L. A. (2002b). Acidophilic character of yeast PID261/BUD32, a putative ancestor of eukaryotic protein kinases. *Biochem. Biophys. Res. Commun.* **296**, 1366-1371.
Facchin, S., Lopreiato, R., Ruzzene, M., Marin, O., Sartori, G., Götz, C., Montenarh, M., Carignani, G. and Pinna, L. A. (2003). Functional homology between yeast piD261/Bud32 and human PRPK: both phosphorylate p53 and PRPK partially complements piD261/Bud32 deficiency. *FEBS Lett.* **549**, 63-66.
Facchin, S., Ruzzene, M., Peggion, C., Sartori, G., Carignani, G., Marin, O., Brustolon, F., Lopreiato, R. and Pinna, L. A. (2007). Phosphorylation and activation of the atypical kinase p53-related protein kinase (PRPK) by Akt/PKB. *Cell. Mol. Life Sci.* **64**, 2680-2689.
Gallant, P. (2009). Drosophila Myc. *Adv. Cancer Res.* **103**, 111-144.
Guertin, D. A. and Sabatini, D. M. (2007). Defining the role of mTOR in cancer. *Cancer Cell* **12**, 9-22.
Hennig, K. M., Colombani, J. and Neufeld, T. P. (2006). TOR coordinates bulk and targeted endocytosis in the Drosophila melanogaster fat body to regulate cell growth. *J. Cell Biol.* **173**, 963-974.
Isotani, S., Hara, K., Tokunaga, C., Inoue, H., Avruch, J. and Yonezawa, K. (1999). Immunopurified mammalian target of rapamycin phosphorylates and activates p70 S6 kinase α in vitro. *J. Biol. Chem.* **274**, 34493-34498.
Kim, E., Goraksha-Hicks, P., Li, L., Neufeld, T. P. and Guan, K. L. (2008). Regulation of TORC1 by Rag GTPases in nutrient response. *Nat. Cell Biol.* **10**, 935-945.
Kisseleva-Romanova, E., Lopreiato, R., Baudin-Baillieu, A., Rousselle, J. C., Ilan, L., Hofmann, K., Namane, A., Mann, C. and Libri, D. (2006). Yeast homolog of a cancer-testis antigen defines a new transcription complex. *EMBO J.* **25**, 3576-3585.
Kozma, S. C. and Thomas, G. (2002). Regulation of cell size in growth, development and human disease: PI3K, PKB and S6K. *Bioessays* **24**, 65-71.
Lee, S. B., Kim, S., Lee, J., Park, J., Lee, G., Kim, Y., Kim, J.-M. and Chung, J. (2007). ATG1, an autophagy regulator, inhibits cell growth by negatively regulating S6 kinase. *EMBO Rep.* **8**, 360-365.
Leevers, S. J., Weinkove, D., MacDougall, L. K., Hafen, E. and Waterfield, M. D. (1996). The Drosophila phosphoinositide 3-kinase Dp110 promotes cell growth. *EMBO J.* **15**, 6584-6594.
Lopreiato, R., Facchin, S., Sartori, G., Arrigoni, G., Casonato, S., Ruzzene, M., Pinna, L. A. and Carignani, G. (2004). Analysis of the interaction between piD261/Bud32, an evolutionarily conserved protein kinase of Saccharomyces cerevisiae, and the Grx4 glutaredoxin. *Biochem. J.* **377**, 395-405.
Marshall, L., Rideout, E. J. and Grewal, S. S. (2012). Nutrient/TOR-dependent regulation of RNA polymerase III controls tissue and organismal growth in Drosophila. *EMBO J.* **31**, 1916-1930.
Meléndez, A. and Neufeld, T. P. (2008). The cell biology of autophagy in metazoans: a developing story. *Development* **135**, 2347-2360.
Miron, M., Verdú, J., Lachance, P. E., Birnbaum, M. J., Lasko, P. F. and Sonenberg, N. (2001). The translational inhibitor 4E-BP is an effector of PI(3)K/Akt signalling and cell growth in Drosophila. *Nat. Cell Biol.* **3**, 596-601.
Miyoshi, A., Kito, K., Aramoto, T., Abe, Y., Kobayashi, N. and Ueda, N. (2003). Identification of CGI-121, a novel PRPK (p53-related protein kinase)-binding protein. *Biochem. Biophys. Res. Commun.* **303**, 399-405.
Montagne, J., Stewart, M. J., Stocker, H., Hafen, E., Kozma, S. C. and Thomas, G. (1999). Drosophila S6 kinase: a regulator of cell size. *Science* **285**, 2126-2129.
Nagel, A. C., Maier, D. and Preiss, A. (2002). Green fluorescent protein as a convenient and versatile marker for studies on functional genomics in Drosophila. *Dev. Genes Evol.* **212**, 93-98.
O'Donnell, A. F., Tiong, S., Nash, D. and Clark, D. V. (2000). The Drosophila melanogaster ade5 gene encodes a bifunctional enzyme for two steps in the de novo purine synthesis pathway. *Genetics* **154**, 1239-1253.
Oldham, S. and Hafen, E. (2003). Insulin/IGF and target of rapamycin signaling: a TOR de force in growth control. *Trends Cell Biol.* **13**, 79-85.

Oldham, S., Montagne, J., Radimerski, T., Thomas, G. and Hafen, E. (2000). Genetic and biochemical characterization of dTOR, the Drosophila homolog of the target of rapamycin. *Genes Dev.* **14**, 2689-2694.
Ollmann, M., Young, L. M., Di Como, C. J., Karim, F., Belvin, M., Robertson, S., Whittaker, K., Demsky, M., Fisher, W. W., Buchman, A. et al. (2000). Drosophila p53 is a structural and functional homolog of the tumor suppressor p53. *Cell* **101**, 91-101.
Peggion, C., Lopreiato, R., Casanova, E., Ruzzene, M., Facchin, S., Pinna, L. A., Carignani, G. and Sartori, G. (2008). Phosphorylation of the Saccharomyces cerevisiae Grx4p glutaredoxin by the Bud32p kinase unveils a novel signaling pathway involving Sch9p, a yeast member of the Akt / PKB subfamily. *FEBS J.* **275**, 5919-5933.
Pelkmans, L., Fava, E., Grabner, H., Hannus, M., Habermann, B., Krausz, E. and Zerial, M. (2005). Genome-wide analysis of human kinases in clathrin- and caveolae/raft-mediated endocytosis. *Nature* **436**, 78-86.
Pullen, N. and Thomas, G. (1997). The modular phosphorylation and activation of p70s6k. *FEBS Lett.* **410**, 78-82.
Purdy, A. and Su, T. T. (2004). Telomeres: not all breaks are equal. *Curr. Biol.* **14**, R613-R614.
Rusten, T. E., Lindmo, K., Juhász, G., Sass, M., Seglen, P. O., Brech, A. and Stenmark, H. (2004). Programmed autophagy in the Drosophila fat body is induced by ecdysone through regulation of the PI3K pathway. *Dev. Cell* **7**, 179-192.
Saltiel, A. R. and Kahn, C. R. (2001). Insulin signalling and the regulation of glucose and lipid metabolism. *Nature* **414**, 799-806.
Sancak, Y., Peterson, T. R., Shaul, Y. D., Lindquist, R. A., Thoreen, C. C., Bar-Peled, L. and Sabatini, D. M. (2008). The Rag GTPases bind raptor and mediate amino acid signaling to mTORC1. *Science* **320**, 1496-1501.
Sancak, Y., Bar-Peled, L., Zoncu, R., Markhard, A. L., Nada, S. and Sabatini, D. M. (2010). Ragulator-Rag complex targets mTORC1 to the lysosomal surface and is necessary for its activation by amino acids. *Cell* **141**, 290-303.
Scott, R. C., Schuldiner, O. and Neufeld, T. P. (2004). Role and regulation of starvation-induced autophagy in the Drosophila fat body. *Dev. Cell* **7**, 167-178.
Scott, R. C., Juhász, G. and Neufeld, T. P. (2007). Direct induction of autophagy by Atg1 inhibits cell growth and induces apoptotic cell death. *Curr. Biol.* **17**, 1-11.
Sherr, C. J. (2004). Principles of tumor suppression. *Cell* **116**, 235-246.
Spradling, A. C. and Rubin, G. M. (1982). Transposition of cloned P elements into Drosophila germ line chromosomes. *Science* **218**, 341-347.
Srinivasan, M., Mehta, P., Yu, Y., Prugar, E., Koonin, E. V., Karzai, A. W. and Sternglanz, R. (2011). The highly conserved KEOPS/EKC complex is essential for a universal tRNA modification, t6A. *EMBO J.* **30**, 873-881.
Stocker, H. and Hafen, E. (2000). Genetic control of cell size. *Curr. Opin. Genet. Dev.* **10**, 529-535.
van Sluijters, D. A., Dubbelhuis, P. F., Blommaart, E. F. and Meijer, A. J. (2000). Amino-acid-dependent signal transduction. *Biochem. J.* **351**, 545-550.
Weinkove, D. D., Neufeld, T. P. T., Twardzik, T. T., Waterfield, M. D. M. and Leevers, S. J. S. (1999). Regulation of imaginal disc cell size, cell number and organ size by Drosophila class I(A) phosphoinositide 3-kinase and its adaptor. *Curr. Biol.* **9**, 1019-1029.
Zhang, H., Stallock, J. P., Ng, J. C., Reinhard, C. and Neufeld, T. P. (2000). Regulation of cellular growth by the Drosophila target of rapamycin dTOR. *Genes Dev.* **14**, 2712-2724.